Optochemical Sensing

DOI: 10.1002/anie.201301045

A Versatile Fiber-Optic Fluorescence Sensor Based on Molecularly Imprinted Microstructures Polymerized in Situ**

*Xuan-Anh Ton, Bernadette Tse Sum Bui, Marina Resmini, Paolo Bonomi, Ihab Dika, Olivier Soppera, and Karsten Haupt**

Molecularly imprinted polymers (MIPs) are tailor-made biomimetic materials that are capable of specific recognition towards an analyte. They are synthesized by co-polymerizing functional and cross-linking monomers in the presence of a molecular template. Subsequent removal of the template leaves complementary binding sites with affinities and specificities comparable to those of natural receptors.[1,2] Their molecular recognition properties, combined with their high stability, robustness, and easy synthesis, make them extremely attractive as sensing materials.[3,4] Therefore they are considered as interesting alternatives to biological recognition elements in biosensors. In this context, MIPs have been widely applied to optical sensing, for example, with fluorescence detection.[5–9]

Herein we describe a new type of fluorimetric sensor based on an optical fiber that carries a micrometer-sized MIP tip photopolymerized in situ at one end. To develop a versatile device, we have used three approaches: 1) a core–shell format of the tip for a faster response; 2) gold nanoparticles for signal enhancement; and 3) fluorescent reporter groups incorporated into the MIP for the detection of nonfluorescent analytes. Optical fibers are of interest as they offer many advantages such as ease of miniaturization and integration, low cost, and limited loss of light. Polymer-based optical fiber sensors have been reported,[10,11] and a few examples of intrinsic MIP-based fiber optic sensors have been developed for detecting nerve agents,[12] cyanotoxins[13] and cocaine.[14] In these examples, the coating of the polymer on the fiber was rather complex, requiring time-consuming multistep procedures, such as pretreatment of the fiber (polishing, surface activation, silanization) before the polymer can be covalently attached. In our system, we use a laser beam emerging from the fiber core to synthesize a polymer microtip at the extremity of the fiber that appears as an extension of the fiber core (Figure 1 A,B).[15] Standard telecommunication optical fibers with an 8 μm core were employed without any prior treatment. The photoinitiator bis(2,4,6-trimethylbenzoyl)phenyl phosphine oxide, which is very reactive towards methacrylates, was used, making the MIP formulations extremely photosensitive.[16,17] This allows very fast polymerization, which was complete in only 10 seconds. Two optical setups were used to demonstrate our sensing concept. In the first setup, excitation is through the fiber and the fluorescence response of the MIP is detected at the tip level by external collection using a fiber optic mini-spectrofluorimeter (Figure 1 B). This setup can be used for example for integration into microfluidic sensor chips. In the second setup, a Y-shaped bifurcated fiber is used; the fluorescent light emitted from the MIP tip upon excitation through one arm of the optical fiber is collected by the fiber and guided through the other arm for detection by a spectrofluorimeter (Figure 1 C). This setup is particularly useful for sensing at long distances and in setups where the light collection cannot be carried out externally.

While fluorescent target analytes can be measured directly, we use two different ways to monitor binding of nonfluorescent targets to the MIP, either in a competitive setup with a fluorescent analogue of the target analyte or by including a fluorescent monomer into the MIP, the fluorescence of which changes upon analyte binding. To demonstrate the first format, a MIP was imprinted with a model template, carbobenzyloxy-L-phenylalanine (*Z*-L-Phe), and binding was monitored with a fluorescent probe, its analogue dansyl-L-phenylalanine (dansyl-L-Phe) (Scheme 1). In the second format, the MIP was imprinted with the herbicide 2,4-dichlorophenoxyacetic acid (2,4-D) as a model target, using the fluorescent monomer *N*-2-(6-(4-methylpiperazin-1-yl)-1,3-dioxo-1*H*-benzo[de]isoquinolin-2(3*H*)-yl-ethyl)acrylamide (FIM) for signaling. Binding was monitored by a change in the fluorescence intensity in both cases. The most crucial step was to develop a MIP formulation combining good recognition properties with polymer photostructuring into a micrometer-sized tip.[18] The formulation was inspired from previous work.[17,19,20] Optimization of the MIP formulation

[*] X. A. Ton, Dr. B. Tse Sum Bui, Prof. K. Haupt
Université de Technologie de Compiègne
Génie Enzymatique et Cellulaire
Rue Roger Couttolenc, CS60319, 60203 Compiègne (France)
E-mail: karsten.haupt@utc.fr
Homepage: http://www.utc.fr/mip
Dr. M. Resmini, Dr. P. Bonomi
School of Biological and Chemical Sciences
Queen Mary University of London
Mile End road, London E1 4NS (UK)
I. Dika, Dr. O. Soppera
Institut de Science des Matériaux de Mulhouse
UMR CNRS 7361, BP 2488, 68057 Mulhouse (France)

[**] The authors acknowledge financial support by the European Union (Marie Curie IAPP IRMED, grant No. PIAP-GA-2009-251307, and European Regional Development Fund), and by the Regional Council of Picardie (CBI-PEM project, and co-funding of equipment under CPER 2007-2013). We thank L. Vidal and T. Bourgade for TEM and confocal microscopy measurements, respectively. XAT thanks CD Ton, D. Ros, and J. Istria for their help with the fiber optics setup.

Supporting information for this article, including experimental details (reagents and materials, synthesis and characterization of the fluorescent monomer FIM, the MIP microtip fabrication process, and binding studies of polymer microtips on the fibers), is available on the WWW under http://dx.doi.org/10.1002/anie.201301045.

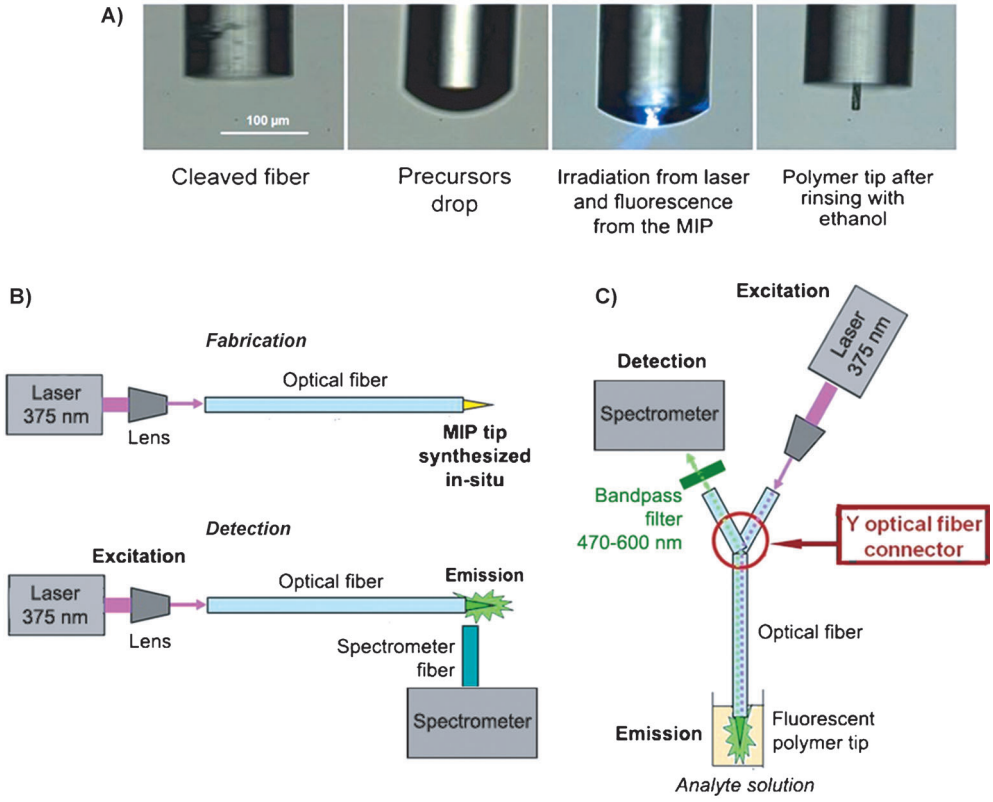

Figure 1. A) The microtip fabrication process. B) Analysis by spectrofluorimetry of the polymer microtips with a simple fiber or C) a bifurcated fiber. A 375 nm diode laser is used both for microtip polymerization and for excitation of the fluorophore.

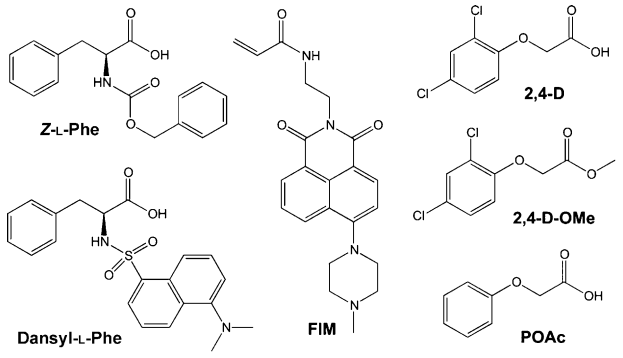

Scheme 1. Chemical structures of compounds used in this study.

(in particular with respect to viscosity and polymerization kinetics) and the photonic parameters (laser power and irradiation time) allowed a stiff and stable MIP microtip to be generated in 10 seconds. The formulation used for the competitive format, termed P1, is described in the Supporting Information, Table S1. It consists of ethylene glycol dimethacrylate (EGDMA) and pentaerythritol triacrylate PETIA (2:1) as cross-linkers and tetraglyme as solvent, the high viscosities of which favored photostructuring of a tip with the desired shape. The length and diameter of the tip produced were 35–40 µm and 15 µm, respectively.

The molecular recognition and sensing properties of the *Z*-L-Phe MIP tip were investigated with the simple optical fiber set-up (Figure 1B). Specific binding was demonstrated by comparing the response of MIP and non-imprinted control polymer (NIP) microtips when incubated with the fluorescently labeled dansyl-L-Phe; an imprinting factor (binding to the MIP/binding to the NIP) of 3.5 was observed (Figure 2, curves (a) and (d)). We assessed the selectivity of our sensor through competitive binding experiments between the fluorescent probe dansyl-L-Phe and the imprinting template *Z*-L-Phe or its opposite enantiomer *Z*-D-Phe. When the sensor was incubated in a mixture of 10 µM dansyl-L-Phe and 10 µM *Z*-L-Phe, the binding of dansyl-L-Phe to the MIP was greatly reduced (Figure 2, curve (b)), whereas if 10 µM of *Z*-D-Phe was used instead, the competition was weaker (Figure 2, curve (c)), which reflects the selectivity of the MIP for the L-enantiomer, the original template.

The concentration dependence of the MIP fluorescence signal was also tested and the limit of detection (LOD) was found to be 1 µM (Figure 3A; Supporting Information, Fig-

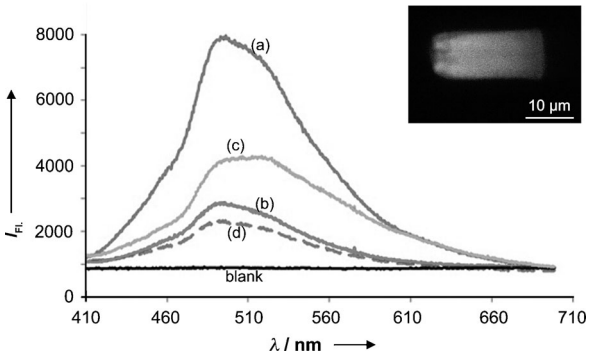

Figure 2. Fluorescence spectra of *Z*-L-Phe-MIP microtips after incubation with a) 10 µM dansyl-L-Phe, b) a mixture of 10 µM dansyl-L-Phe and 10 µM Z-L-Phe, and c) a mixture of 10 µM dansyl-L-Phe and 10 µM Z-D-Phe, in acetonitrile (MeCN). d) Fluorescence spectrum of the NIP microtip after incubation with 10 µM dansyl-L-Phe in MeCN. Blank line: *Z*-L-Phe MIP microtip before incubation. Inset: confocal fluorescence microscopy image of the MIP microtip after incubation with dansyl-L-Phe.

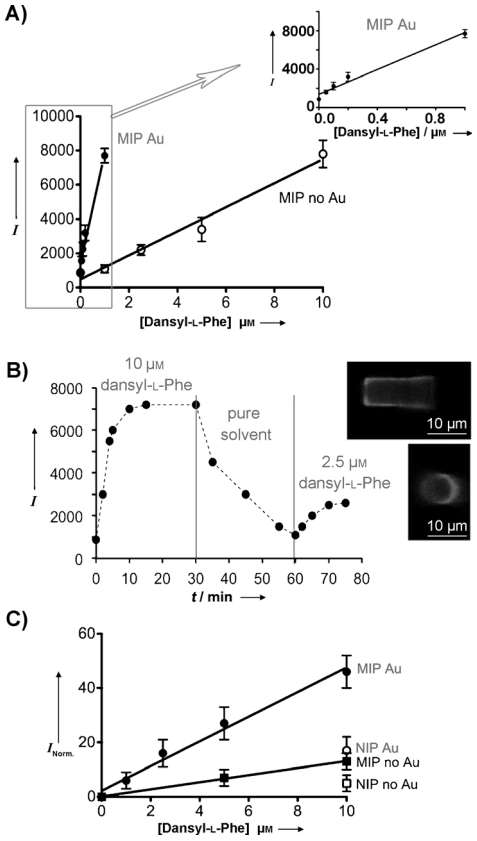

Figure 3. A) Simple fiber: Fluorescence responses of the *Z*-L-Phe MIP tip without gold ("MIP no Au", $\lambda_{EM} = 495$ nm) and the composite gold–MIP tip ("MIP Au", $\lambda_{EM} = 489$ nm) after incubation with increasing concentrations of dansyl-L-Phe in MeCN. Integration time: 100 ms. B) Kinetics of the fluorescence response of the core-shell *Z*-L-Phe MIP tip incubated with dansyl-L-Phe. Inset: confocal fluorescence images of the core–shell MIP tip after incubation. C) Bifurcated fiber: Normalized fluorescence responses of the MIP and NIP tips without gold ("MIP no Au" and "NIP no Au", $\lambda_{EM} = 495$ nm) and of the gold composite tips ("MIP Au" and "NIP Au", $\lambda_{EM} = 489$ nm), incubated with increasing concentrations of dansyl-L-Phe in MeCN. Experiments were performed in triplicate; errors bars represent standard deviations. The blank signal was recorded before each set of experiments.

ure S1A). To lower the LOD, we attempted to use the plasmonic enhancement properties of noble-metal nanoparticles to increase the fluorescence signal.[21] Commercial octanethiol-stabilized gold nanoparticles (diameter: 10 nm, dynamic light scattering in Supporting Information, Figure S2) were added to the MIP precursors solution, resulting in a composite gold nanoparticle–MIP microtip. The effective incorporation of Au into the MIP was verified by energy dispersive X-ray spectroscopy and transmission electron microscopy (Supporting Information, Figures S3, S4). The presence of gold nanoparticles effectively led to an enhancement of the optical signal, increasing the sensitivity and lowering the LOD by a factor of 20, to 50 nM (Figure 3A; Supporting Information, Figure S1). Despite the large increase in sensitivity, we presently have no clear evidence for plasmonic enhancement effectively taking place. To the best of our knowledge, this is the first description of MIP sensors using metal-enhanced fluorescence intensity measurements. However, we cannot exclude that a more efficient collection of fluorescent light that is due to scattering by the gold nanoparticles back into the fiber contributes to the observed effect.

The response time of this sensor was 45 min, which is due to analyte diffusion into the tip. The response time could be shortened by using a core–shell format of the tip that results in shorter diffusion distances. We synthesized a nonporous poly(PETIA) core tip covered by a 0.7 μm thin layer of *Z*-L-Phe MIP through reinitiation with the MIP precursors (Figure 3B, inset). Kinetics data of the response of the core–shell MIP tip incubated with 10 μM dansyl-L-Phe in MeCN is shown in Figure 3B. As a result, binding to dansyl-L-Phe could be detected after only 2 min, and around 80% of the total signal response occurred within 4 min. The core–shell MIP tip took around 10 min to reach equilibrium (>95%). Therefore, by reducing the MIP thickness, the response time was successfully lowered from 45 min to 10 min. The reversibility of the sensor response was also demonstrated by measuring successively different concentrations of dansyl-L-Phe (Figure 3B), which indicates that fluorescent analytes could be measured close to real-time and without intermittent regeneration (although this is not possible in the competitive format).

Sensing experiments were also performed with the bifurcated fiber setup (Figure 1C), thus allowing long-distance measurements and real-time detection. In this configuration, interference by fluorescent components of the sample matrix other than the target analyte are minimized. The specificity, the concentration-dependence of the fluorescence response of the MIP, and the fluorescence enhancement induced by gold nanoparticles were confirmed as well for the bifurcated fiber (Figure 3C).

To avoid the addition of a fluorescent probe as in the competitive format and to broaden the applicability of the sensor, we incorporated fluorescent reporter groups into the MIP, a concept that has been developed by Takeuchi.[22,23] The herbicide 2,4-D, our model analyte, is widely used; it represents a threat for health owing to its endocrine disruption properties.[24] To detect 2,4-D, a fluorescent functional monomer based on a piperazinyl naphthalimide derivative was synthesized (FIM; see the Supporting Information). FIM exhibits fluorescence amplification owing to the protonation of the piperazinyl residue upon interaction with carboxyl groups,[25] here 2,4-D ($pK_a = 5.09$, methanol/water 4:1), which was verified through fluorescence titration experiments (Supporting Information, Figure S5). Very recently, a MIP containing a naphtalimide for sensing purposes has been reported. The naphthalimide monomer was different, though, and used fluorescence quenching for detection, resulting in sensitivity in the mM range.[26] FIM was incorporated into a 2,4-D MIP formulation adapted from Haupt et al.,[27] replacing part of the 4-vinylpyridine functional monomer of the original procedure. We verified using a MIP synthesized in the form of nanoparticles and batch binding assays that the performances of the new 2,4-D MIP were similar to those of the earlier MIP (not shown). The MIP was synthesized at the end of an optical fiber, using the core–shell format (P2; Supporting Information, Table S1). The

specific recognition properties were demonstrated by incubating both MIP and NIP microtips with increasing concentrations of 2,4-D. The fluorescence response of the MIP was concentration-dependent, with a LOD of 2.5 nM (50 times lower than the tolerated amount in drinking water of 30 $\mu g L^{-1}$, that is, 135 nM, recommended by the World Health Organization[28]), and the MIP yielded a higher signal than the NIP (Figure 4A). For instance, when incubated with 2.5 nM 2,4-D, the MIP tip increased in fluorescence by around 20%, while the NIP intensity increased by only 5% (Supporting Information, Figure S6). The 2,4-D MIP tip attained a stable response within 5 min of incubation. The dynamic response and reversibility of the MIP-based sensor were also demonstrated by consecutively measuring various concentrations of 2,4-D (Supporting Information, Figure S7).

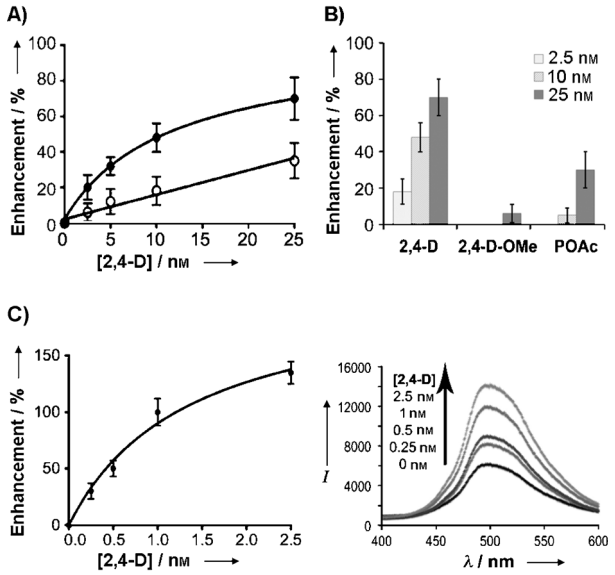

Figure 4. A) Fluorescence enhancement responses of MIP and NIP microtips after incubation with increasing concentrations of 2,4-D in methanol/water (4:1). Spectrometer integration time: 600 ms. B) Fluorescence signal of the 2,4-D MIP microtip after incubation with 2,4-D or the analogues 2,4-D-OMe or POAc in methanol/water (4:1). C) Fluorescence signal of the composite gold-MIP P2 microtip after incubation with increasing concentrations of 2,4-D in methanol/water (4:1). Integration time: 50 ms. Experiments were performed in triplicate; errors bars represent standard deviations. The blank signal (tip before incubation) was recorded before each set of experiments.

The selectivity of MIP was evaluated by measuring the responses to two structurally related compounds, 2,4-dichlorophenoxyacetic acid methyl ester (2,4-D-OMe), the carboxyl group of which is blocked, and phenoxyacetic acid (POAc, $pK_a = 5.17$, methanol/water 4:1), lacking the ring chlorine atoms. As a result, a smaller fluorescence enhancement for POAc and no enhancement for 2,4-D-OMe were observed, thus confirming the selectivity of the MIP for 2,4-D (Figure 4B). Non-related molecules containing a carboxyl group, such as glucuronic acid ($pK_a = 5.22$, methanol/water 4:1) and Z-L-Phe ($pK_a = 5.06$, methanol/water 4:1) generated no response, although they do interact with FIM, as verified through fluorescence titration (not shown).

To further increase the sensitivity of our sensor, we again incorporated gold nanoparticles into the MIP formulation, which led to a stronger fluorescence enhancement upon binding, lowering the LOD to 0.25 nM (Figure 4C). This is lower than the more restrictive limit concentration for pesticides in drinking water set by the European Union (0.1 $\mu g L^{-1}$, that is, 0.45 nM.[29]) Thus the sensitivity of our sensor is comparable to that obtained with chromatography/mass spectrometry for 2,4-D detection.[28,30,31]

In conclusion, we have developed a versatile fluorimetric fiber optic sensor using in situ polymerized MIP microstructures as recognition element, which were generated in only a few seconds. The sensitivity of the sensor was significantly improved by exploiting the effect of signal enhancement induced by gold nanoparticles embedded in the polymer. A detection limit as low as 250 pM for the herbicide 2,4-D, which is comparable to that of LC/MS techniques, was achieved. The use of a signaling monomer in the MIP is an advantage as it simplifies the detection method for nonfluorescent analytes. The fact that fluorescence is enhanced rather than quenched is an additional advantage, as non-specific quenching resulting in false-positive responses is avoided. This method is applicable to other analytes carrying carboxyl groups, and, we believe, with different signaling monomers to a wider range of analytes. These studies pave the way to the miniaturization of compact portable MIP-based fiber optic sensors for the real-time remote detection of environmental and other analytes.

Received: February 5, 2013
Revised: April 4, 2013
Published online: June 21, 2013

Keywords: fluorescent probes · metal-enhanced fluorescence · optical fibers · polymers · sensors

[1] R. Arshady, K. Mosbach, *Makromol. Chem.* **1981**, *182*, 687–692.
[2] G. Wulff, A. Sarhan, *Angew. Chem.* **1972**, *84*, 364; *Angew. Chem. Int. Ed. Engl.* **1972**, *11*, 341–342.
[3] G. Wulff, *Angew. Chem.* **1995**, *107*, 1958–1979; *Angew. Chem. Int. Ed. Engl.* **1995**, *34*, 1812–1832.
[4] K. Haupt, K. Mosbach, *Chem. Rev.* **2000**, *100*, 2495–2504.
[5] P. Turkewitsch, B. Wandelt, G. D. Darling, W. S. Powell, *Anal. Chem.* **1998**, *70*, 2025–2030.
[6] F. L. Dickert, H. Besenböck, M. Tortschanoff, *Adv. Mater.* **1998**, *10*, 149–151.
[7] S. Al-Kindy, R. Badía, J. L. Suárez-Rodríguez, M. E. Díaz-García, *Crit. Rev. Anal. Chem.* **2000**, *30*, 291–309.
[8] O. Y. F. Henry, D. C. Cullen, S. A. Piletsky, *Anal. Bioanal. Chem.* **2005**, *382*, 947–956.
[9] X. A. Ton, V. Acha, K. Haupt, B. Tse Sum Bui, *Biosens. Bioelectron.* **2012**, *36*, 22–28.
[10] X. D. Wang, O. S. Wolfbeis, *Anal. Chem.* **2013**, *85*, 487–508.
[11] J. E. Epstein, D. R. Walt, *Chem. Soc. Rev.* **2003**, *32*, 203–214.
[12] A. L. Jenkins, O. M. Uy, G. M. Murray, *Anal. Chem.* **1999**, *71*, 373–378.
[13] R. B. Queirós, S. O. Silva, J. P. Noronha, O. Frazão, P. Jorge, G. Aguilar, P. Marques, M. G. F. Sales, *Biosens. Bioelectron.* **2011**, *26*, 3932–3937.
[14] T. H. Nguyen, S. A. Hardwick, T. Sun, K. T. V. Grattan, *IEEE Sens. J.* **2012**, *12*, 255–260.

[15] O. Soppera, S. Jradi, D. J. Lougnot, *J. Polym. Sci. Part A* **2008**, *46*, 3783 – 3794.
[16] Z. Szablan, T. Junkers, S. Koo, T. Lovestead, T. Davis, M. Stenzel, C. Barner-Kowollik, *Macromolecules* **2007**, *40*, 6820 – 6833.
[17] Y. Fuchs, A. V. Linares, A. G. Mayes, K. Haupt, O. Soppera, *Chem. Mater.* **2011**, *23*, 3645 – 3651.
[18] Y. Fuchs, O. Soppera, K. Haupt, *Anal. Chim. Acta* **2012**, *717*, 7 – 20.
[19] O. Ramström, L. I. Andersson, K. Mosbach, *J. Org. Chem.* **1993**, *58*, 7562 – 7564.
[20] S. Piperno, B. Tse Sum Bui, K. Haupt, L. A. Gheber, *Langmuir* **2011**, *27*, 1547 – 1550.
[21] a) J. Zhang, J. R. Lakowicz, *Opt. Express* **2007**, *15*, 2598 – 2606; b) K. Toma, J. Dostalek, W. Knoll, *Opt. Express* **2011**, *19*, 11090 – 11099.
[22] J. Matsui, Y. Tachibana, T. Takeuchi, *Anal. Commun.* **1998**, *35*, 225 – 227.
[23] T. Takeuchi, T. Mukawa, H. Shinmori, *Chem. Rec.* **2005**, *5*, 263 – 275.
[24] J. S. Bus, L. E. Hammond, *Crop Prot.* **2007**, *26*, 266 – 269.
[25] C. G. Niu, G. M. Zeng, L. X. Chen, G. L. Shen, R. Q. Yu, *Analyst* **2004**, *129*, 20 – 24.
[26] R. Wagner, W. Wan, M. Biyikal, E. Benito-Peña, M. C. Moreno-Bondi, I. Lazraq, K. Rurack, B. Sellergren, *J. Org. Chem.* **2013**, *78*, 1377 – 1389.
[27] K. Haupt, A. Dzgoev, K. Mosbach, *Anal. Chem.* **1998**, *70*, 628 – 631.
[28] *Guidelines for drinking-water quality*, 4th ed., World Health Organization WHO, Geneva, **2011**, pp. 347 – 348.
[29] Council Directive 98/83/EC of 3 November 1998 on the quality of water intended for human consumption http://eur-lex.europa.eu/LexUriServ/LexUriServ.do?uri=CELEX:31998L0083:EN:NOT.
[30] M. Shamsipur, N. Fattahi, M. Pirsaheb, K. Sharafi, *J. Sep. Sci.* **2012**, *35*, 2718 – 2724.
[31] W. H. Ding, C. H. Liu, S. P. Yeh, *J. Chromatogr. A* **2000**, *896*, 111 – 116.

